Journal of Food Measurement and Characterization (2021) 15:585–593
https://doi.org/10.1007/s11694-020-00669-w

ORIGINAL PAPER

Active barrier chitosan films containing gallic acid based oxygen scavenger

Gaurav Singh[1] · Suman Singh[2] · Bijender Kumar[3] · Kirtiraj K. Gaikwad[1]

Received: 29 July 2020 / Accepted: 15 September 2020 / Published online: 21 September 2020
© Springer Science+Business Media, LLC, part of Springer Nature 2020

Abstract

Active oxygen barrier films of chitosan/gallic acid/sodium carbonate (CH/GA/SC) were prepared by solution casting method. The effect of gallic acid on physical, mechanical, structural, and oxygen scavenging properties of films was investigated. As compared with neat CH film, CH/GA/SC films displayed higher thicknesses and water solubility. Tensile strength and elongation at break were affected by the addition of gallic acid and sodium carbonate. The chemical interaction evaluated by Fourier-transform infrared spectroscopy and morphology evaluated by scanning electron microscopy, and it is noticed that sodium carbonate and gallic acid were distributed homogeneously in the film structure. The X-ray diffraction confirmed that gallic acid, sodium carbonate, and chitosan had excellent compatibility. The addition of gallic acid in the chitosan matrix caused low water and oxygen permeability. The lowest oxygen transmission rate of the film was 4.10 ± 1.07 $cm^3/\mu m/m^2$ day kpa. The CH/GA/SC 20 film displayed the maximum oxygen-absorbing rate and capacity of 2.66 mL O_2/g. day and 19.55 mL O_2/g respectively, at 23 ± 2 °C. Moisture inside the package was utilized as a catalyst to begin the oxygen scavenging reaction. The results suggest that the combination of gallic acid and the sodium carbonate in chitosan film is a promising oxygen scavenging material for active oxygen barrier films.

Keywords Chitosan · Film · Oxygen barrier · Gallic acid · Active packaging · Oxygen scavenging film

Introduction

In recent years, the acceptance of plastic as packaging materials that deliver better protection to their product, especially in the food and pharmaceutical sector, is speedily growing [1, 2]. The research studies on biodegradable films based on biopolymers have been studied widely for food packaging applications. These bio packaging materials have been known for enhancing environmental sustainability and for important technical properties that are essential to broadly achieve food packaging roles [3–6]. The extensive use of polymeric materials in the packaging applications has encouraged debates about their sufficient ability to slow down and block the water vapours and oxygen diffusion that are the principal reason for the short of the storage life of the packed processed food [7–10].

In maximum cases, the storage life of food products affected by the presence of oxygen [11, 12]. An extensive number of food products, especially lipid-based, are susceptible to oxidative damage and hence change in color, taste, texture, browning, and bleaching of the food product [13]. The development of rancidity in especially in the high fat-containing food products is widespread. Aerobic microbial growth due to oxygen can be an issue in raw meat products and seafood as well as high water activity food [9, 10, 14]. Low concentration (in the range of 1–200 ppm) of oxygen may reason considerable nutritional losses in food products. The concentration of remaining oxygen is much higher in most packages; hence, it is vital to avoid the access of oxygen in the package during the filling process. The diffusion of oxygen through the package wall is the process of

✉ Kirtiraj K. Gaikwad
kirtiraj.gaikwad@pt.iitr.ac.in

[1] Department of Paper Technology, Indian Institute of Technology Roorkee, Roorkee, Uttarakhand 247667, India

[2] Department of Food Engineering, Institute of Food Science & Technology, VCSG Uttarakhand University of Horticulture and Forestry, Majri Grant, Dehradun, Uttarakhand 248140, India

[3] Creative Research Centre for Nanocellulose Future Composite, Department of Mechanical Engineering, Inha University, 253 Yonghyun-dong, Incheon 402751, Republic of Korea

permeability in the polymeric packaging material [4, 15]. To overcome such oxygen permeability issues, appropriate packaging materials which can be utilized for food packaging by combining passive oxygen barrier layers with active oxygen barrier layers, such as oxygen absorber layers using oxygen absorber. Currently, numerous techniques occur, which allows the integration of oxygen absorber into the packaging materials, in the majority of the cases, as separate elements (sachets). The use of sachets in packages is not permitted in all countries, and therefore novel methods are required so to ensure significantly higher oxygen barrier as well as scavenging properties by packaging materials [3, 9].

Commercial application address permeability issues employing laminated polymeric films, comprising five to nine layers to achieve substantial oxygen barrier necessities. Polymeric films having a passive barrier layer avoid oxygen permeation from the external environment of the package, but do not eliminate oxygen contained in the package [16]. Since biodegradable polymers usually have weak oxygen barrier, high-performance flexible packages involving them are usually multilayer. Synthetic polymers such as polyethylene vinyl alcohol, polyamides, or polyvinyl dichloride were usually used with biodegradable polymers in multilayer structures to achieve the desired permeability of films. However, this solution limits their recyclability, structures, and their biodegradability (or compost ability) of biodegradable polymers [17]. The development of biodegradable polymers films with high barrier properties enables them to be degraded/composted hence improving the sustainability and carbon footprint of products.

Gallic acid (GA) is a plant-based polyphenolic compound with 3-hydroxy groups (OH) and very soluble in the aqueous stage, act as a crosslinking agent and antioxidant and hence it is generally utilized to inhibit oxidation process in food products [9, 18]. GA absorbs a high amount of oxygen when exposing to the alkaline environment; therefore, it is essential that the GA combined with an alkaline compound. GA oxidizes with the development of hydrogen peroxide (H_2O_2), quinones, and semi-quinones in an alkaline condition [8]. Hence, GA is an active natural compound as an oxygen absorber [19]. Apart from the oxygen scavenging properties GA also showed plasticizing properties when incorporated into a biopolymer; therefore, it improved elasticity in the film [20].

The present study focus on the enhancement of the active oxygen barrier properties of chitosan film by developing active oxygen barrier layers using oxygen scavenger. Hence a chitosan films was prepared with incorporation of 3, 5, 10, and 20% gallic acid and sodium carbonate. The active oxygen barrier and oxygen scavenging properties (rate and capacity) of the active CH/GA/SC films were studied. We also assessed the surface microstructure, physicochemical interface, mechanical, and surface color properties of the prepared active CH/GA/SC films.

Materials and methods

Materials

Chitosan monohydrate (Deacetylation: 75–85%, M_V = 8.0×10^5 Da) was purchased from Sigma Aldrich (Mumbai, India). Glycerol (Pure pharmaceutical grade) as a plasticizer, Acetic acid (1 N) as a solvent, and Sodium Carbonate (anhydrous, 99.5%) were purchased from HiMedia chemicals (Mumbai, India). Gallic acid (98% Assay) supplied by BioGen Chemicals (P) Ltd. (New Delhi, India).

Preparation of active barrier films

Chitosan-based active barrier films were developed by utilizing the polymer solution casting method, as suggested by Zarandona et al. [21], with few alterations. First, 1% (w/v) of chitosan powder was well dissolved in 1 wt% acetic acid solvent solution and kept at 27 ± 2 °C with continuous magnetic stirring for about 1 h. Subsequently, 0, 1, 5, 10, and 20 wt% GA (chitosan-based) and sodium carbonate (2:1 ratio based on GA) added, and magnetic stirring till fully dissolved to get the film-forming solution. Further, 20 wt% glycerol (chitosan-based) as a plasticizer was poured into a film-forming solution. The obtained solution was stirred at 30 ℃ for 40 min to obtain a homogeneous film-forming solution. The homogenized solution was then poured (40 mL) into petri plates to retain the uniformed thickness (63.09 ± 5.21 µm) and left to dry at 27 ± 2 °C for 48 h. The absence of GA in the CH film was developed and labelled as Neat CH. The chitosan films incorporated with GA and sodium carbonate (SC) were labelled as CH/GA/SC 1, CH/GA/SC 5, CH/GA/SC 10, and CH/GA/SC 20 as a role of gallic acid and sodium carbonate presence. All obtained CH/GA/SC films were conditioned in an environmental chamber (CIATS, Toaps Co., New Delhi) at 25 °C and 50% relative humidity (RH) prior to physical, mechanical analysis.

Characterization of films

Thickness of prepared films

The thickness of prepared CH/GA/SC films was evaluated employing a portable digital micrometer (MITUTOYO 293-821-30, Kobe, Japan). Thickness measurements of films were taken at seven random positions of each CH/GA/SC film, and the mean value of the film for thickness was calculated.

Surface color of films

Color of prepared CH/GA/SC films refers to the method described by Gaikwad et al. [22]. utilizing a Minolta Chroma Meter (CR-400, Konica Minolta Co., Tokyo, Japan). The white plate (L = 86.40, a = 3.1, and b = 2.41) was employed as the standard for the analysis. Color of prepared films was stated as *L** (lightness), *a** (redness/greenness) and *b** (yellowness/blueness) values. *seven random positions of the* films were chosen and evaluated with Chroma Meter. The total color difference (ΔE) of CH/GA/SC films was calculated by using the following Eq. 1.

$$\Delta E = \left(\Delta L^2 + \Delta a^2 + \Delta b^2\right)^{0.5} \quad (1)$$

where ΔL = L standard – L test sample, Δa = a standard – a sample, and Δb = b standard – b sample.

Fourier transform infrared spectroscopy

Fourier transform infrared spectroscopy (FTIR) was performed to analyse the structural interactions of chitosan films impregnated with SC and GA. FTIR spectra of prepared films was noted on a PerkinElmer FTIR spectrophotometer (Chicago, USA) with 32 scans and 4 cm^{-1} resolution. All scans were performed at room temperature (25 °C) between the frequency range of 4000–400 cm^{-1} through a resolution of 4 cm^{-1}.

Scanning electron microscopy

Morphological study of CH/GA/SC film surfaces was explored utilizing a scanning electron microscope (SEM) (LEICA S 360, Leica Cambridge Ltd., NY, USA) with an accelerating voltage of 10 to 15 kV. Before imaging, all film samples were mounted on aluminium stubs coated with a thin layer of gold to get the sample more conductive.

Mechanical properties of films

The mechanical properties, in particular, tensile strength (TS) and elongation at break (EB) of the prepared CH/GA/SC film test samples were analyzed as per standards suggested by ASTM method D882-02 with a Universal Testing Machine (Instron-1195, Bangalore Integrated System Solutions, Bengaluru, India). All tasters were prepared in a rectangular shape (3 × 10 cm). Preliminary grip separation was set at 50 mm, and the speed of the crosshead was set at 0.8 mm/s. A similar test was repeated for seven times for each test sample to authorize its repeatability.

Water solubility of films

The solubility of CH/GA/SC films in water measured by following the method described by Wang et al. [23]. The CH/GA/SC films, earlier conditioned at 75% RH and were shaped into strips (1 cm × 4 cm), further dipped into 50 mL of deionized water and well stirred at 150 rpm. Subsequently, after 24 h, test samples were taken out from deionized water and well dried out at 110 °C for about 24 h final dry weight (W_f) was noted. The primary dry weight of film (W_i) was evaluated by exposure of strips to air in a hot air oven at 110 °C till constant weight. These tests were performed in triplicate, and the average value was taken. The solubility of CH/GA/SC films in water was calculated as per the following Eq. 2.

$$WS(\%) = \frac{Wi - Wf}{Wi} \times 100 \quad (2)$$

X-ray diffraction analysis

X-ray patterns of the CH/GA/SC films were observed utilizing an X-ray diffractometer (D4 PHASER, Madrid, Spain) with Ni-filtered Cu Kα radiation (40 kV, 30 mA). The test samples were scanned between $2\theta = 3–40°$ with a scanning speed of 2° min^{-1}. Before analysis, the test samples were thoroughly dried in a hot air oven and further kept in a desiccator until testing.

Water vapor permeability (WVP)

The WVP of the CH/GA/SC active barrier films was evaluated according to standard method ASTM 1249 employing an L80 water vapor permeation tester (TSY-W3, Labthink Instruments Co., Ltd. China). The CH/GA/SC films were exposed to 23 °C, and 55% RH and the water vapor transmission rate (WVTR) values were determined by means of phosphorus pentoxide (P_2O_5) humidity sensor. The water vapor permeability coefficient of CH/GA/SC was calculated by using the following Eq. 3.

$$WVP\left(\mathrm{g\,mm/m^2\,h\,kPa}\right) = \frac{WVTR \cdot T}{\Delta p} \quad (3)$$

Here, WVTR is the rate at which water vapor transmits through the film (g/m^2 h); T is mean film thickness (mm); Δp is the partial pressure difference across the film (kPa). For all samples, the test was carried out in triplicates, and the mean values were reported.

Oxygen permeability (OP) after activation of film

The oxygen permeability of CH/GA/SC films was evaluated at 25 °C and 55% RH by using Oxygen permeation tester (OX2/230 Intertek, London, UK) by means of O_2 as

the test gas. The oxygen infusion chamber was divided into 2 sections by a CH/GA/SC film. The oxygen in both chambers was expatriated unceasingly for at least 12 h before the evaluation was started. Then, the O_2 was occupied in the upstream chamber. The pressure differences in the downstream chamber were noted versus time. All films were activated for the oxygen scavenging reaction before the test and tested in triplicate, and the average value was reported.

$$OP\left(\text{g mm/m}^2\,\text{day kPa}\right) = \frac{OTR \cdot T}{\Delta p} \quad (4)$$

Here, OTR: oxygen transmission rate (cc/m/day); T: the thickness of the film (mm); ΔP: partial pressure difference across the film (kPa).

Oxygen-scavenging properties of films

Oxygen scavenging properties of CH/GA/SC was evaluated by determining the oxygen concentration in the headspace as a function of time. The absorption cell utilized for the oxygen absorption evaluation, as presented in Fig. 1 comprises of a 250 mL glass flask holding two pieces (8 × 6 cm) and 5.0 g w/w prepared CH/GA/SC films with air (20.9% oxygen). The glass flask was prepared with 10 mL of water to produce 95% RH. The sensor sticker was attached to the wall of the glass flask then closed with an airtight rubber stopper. The glass flask was kept at ambient temperature (23 ± 2 °C) for 8 days. The storage condition (temperature and RH) for glass flask were preserved during the test (8 days), and oxygen concentration was regularly analysed by using an OpTech optical fluorescence oxygen analyzer (MOCON Inc. Chicago, IL, USA).

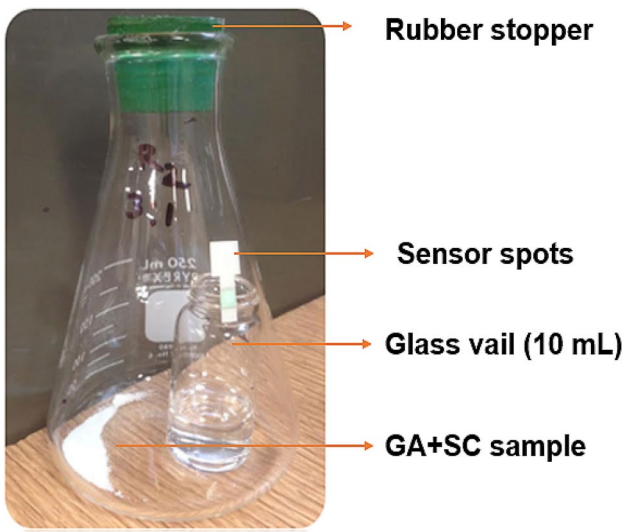

Fig. 1 Airtight absorption cell with a PTFE septum

Statistical treatment

In this study, all the experiments were performed in three replications. The analysis of the data was done using two-way ANOVA, based on a completely randomized simple design and using Minitab software version 16.2.4. The comparisons of means were made using Tukey's test at a 95% confidence level ($p < 0.05$). The graphs were drawn using Sigma plot software version 2010.

Results and discussion

Thickness

The thicknesses of CH/GA/SC films increased from 0.038 to 0.048 mm with the addition of GA and SC in CH film, as presented in Table 2. The CH/GA/SC films were significantly thicker ($p < 0.05$) compared to Neat CH film. The thickness of CH/GA/SC 1 film was close to Neat CH film, displaying no significant difference compared to Neat CH ($p > 0.05$). Results proposed that the increased amount of GA and SC into CH films, thicknesses of films were increased. This might be a result of the effect of GA, which incorporated into the inside network of CH films, in addition to the higher solid content in CH films (24, 22). Our results are in good agreement with the results described by Rezaee et al. [24].

Surface color

From a commercial standpoint, the color parameters of polymeric packaging material might affect the presence of packaging film, which further impacts the acceptance of packaged products to consumers. The hunter lab values (L^*, a^*, and b^*) of prepared CH/GA/SC films are presented in Table 1. The neat CH films with the absence of sodium carbonate and gallic acid displayed the highest darkness (lowest L^* value). The L^* values for Neat CH film and CH/GA/SC 20 were 29.03 ± 0.02 and 56.12 ± 0.77, respectively. With the increasing of SC and GA content, the increased value of lightness, which indicated the film became more color less and more transparent, and the increased values of a^* and b^* designated the color of prepared film inclined to whiteness. The alteration in color in the prepared films was most likely produced by the phenolic compound present in GA. Phenolic content incorporated into films, credited to chemical moieties, and the number of color pigments existing in polyphenolic compounds [8]. Apart from GA, SC played a vital role in the changes in the color of the film. Our results agree with those of Ahn et al. [8], who reported that the

Table 1 Color, Oxygen permeability of activated films, WVP and water solubility values of CH/GA/SC films containing different concentrations of gallic acid

Sample	*L*	Colour *a*	*b*	Oxygen permeability of activated films (cm^3/um/m^2.day.kpa)	WVP (g mm/m^2 h kPa)	Water solubility (%)
Neat CH	29.03 ± 0.02^a	-2.12 ± 0.02^a	2.87 ± 0.01^a	6.21 ± 1.23^a	3.54 ± 1.23^a	22.65 ± 0.71^a
CH/GA/SC 1	33.11 ± 0.02^a	-2.31 ± 0.02^a	2.73 ± 0.03^a	6.19 ± 0.44^a	3.11 ± 0.28^a	22.81 ± 0.29^a
CH/GA/SC 5	39.23 ± 0.34^a	-1.95 ± 0.34^a	4.35 ± 0.11^{ab}	5.77 ± 1.99^b	3.09 ± 0.87^b	26.03 ± 1.44^b
CH/GA/SC 10	48.86 ± 2.21^b	-1.65 ± 0.19^b	6.33 ± 0.81^c	4.23 ± 0.12^c	2.76 ± 0.51^c	29.73 ± 2.01^b
CH/GA/SC 20	56.12 ± 0.77^c	-1.11 ± 0.12^c	7.79 ± 1.24^c	4.10 ± 1.07^c	2.31 ± 0.91^c	32.56 ± 0.84^c

Values are expressed as mean ± standard deviation

Different letters in the same column indicate significant differences ($p < 0.05$)

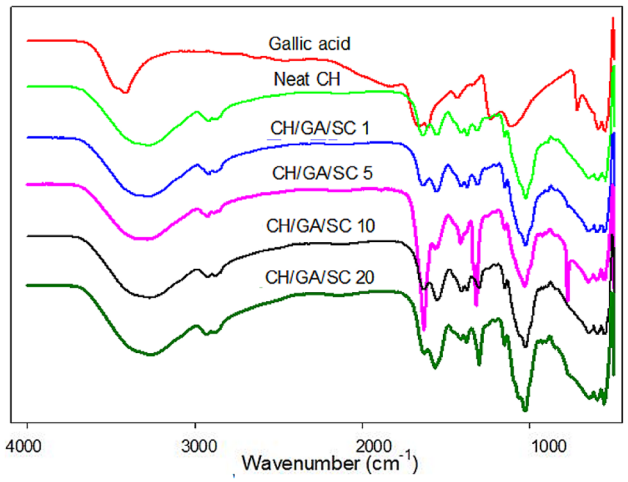

Fig. 2 Fourier transform infrared spectra of chitosan films containing sodium carbonate and gallic acid

color parameter of LDPE films was altered when an oxygen scavenging system containing gallic acid and alkaline compound incorporate into the film.

FTIR

The FTIR spectra of Neat CH and CH/GA/SC films incorporated with SC and GA were presented in Fig. 2. To help the coupling reaction with important amine functional groups present in CH, the carboxylic group (–COOH) of GA is activated by changing the carboxylic acid group (R–COOH) into an ester, as described earlier (Sun et al. 2014). The CH/GA/SC films displayed comparable FTIR spectra as the Neat CH film as a result of the chemical resemblances between starch and cellulose, where the broadband at 3200–3600 cm^{-1} (associated to O–H stretching) and near 2910 cm^{-1} (associated to C–H stretching) was noticed prepared films. A substantial alteration between Neat CH and CH incorporated with GA/SC can be noticed around peaks at 1664 and 1700 $cm^{-1,}$ which shows stretching of carbonyl group present in the chitosan and gallic acid and deformation of amide and amine functional group respectively [25]. Spotted ester and amide links are associated with either GA or CH independently [26]. The spectra of GA displayed numerous characteristic bands between 1400 and 1600 cm^{-1}, associated with the stretching of C=C of conjugated GA [27]. The main differences between the Neat CH and the film CH/GA/SC films were found between 1655 cm^{-1} to 1240 cm^{-1}. In this scale, two bands displayed around 1670 cm^{-1} and 1540 cm^{-1}, associated with the amide (I) and II bands of CH, respectively [21]. Specifically, the band associated with amide (II) was shifted liable on the incorporation of glycerine or GA. Moreover, the band linked to the C–O stretching vibration, which displayed at 1310 cm^{-1} in GA, moved to 1340 cm^{-1} for CH/GA/SC films, indicating the strong interactions among GA and CH.

SEM analysis

Figure 3 displays the morphological images (SEM) of Neat CH and CH/GA/SC active barrier films. The dense structure of the Neat CH and active CH/GA/SC films was noticed. The homogenous and comparatively smooth surface was noticed for Neat CH film. For CH/GA/SC films, the rough surface was observed with the addition of GA and SC into CH. This results due to the heterogeneous film solution of CH/GA/SC compare to the CH film solution [27]. Results indicate that the film-forming solution of chitosan and glycerol (as a plasticizer), GA, and SC homogenous in these films. For CH/GA/SC 5, 10, and 20 films, the presence of a white spot due to heterogeneity in the CH structure when GA and SC were added into the CH solution [25]. They might be SC and GA crystals or by-products as a result of the affinity interface between SC, GA, and CH. Our results are in good agreement with Sun et al. [28], who stated that white spots observed in SEM images when gallic acid incorporation into chitosan-based film-forming solution. Furthermore, rough surfaces of CH/GA/SC due to the conjugation of hydrophilic gallic acid into chitosan which may absorb excessive water molecules

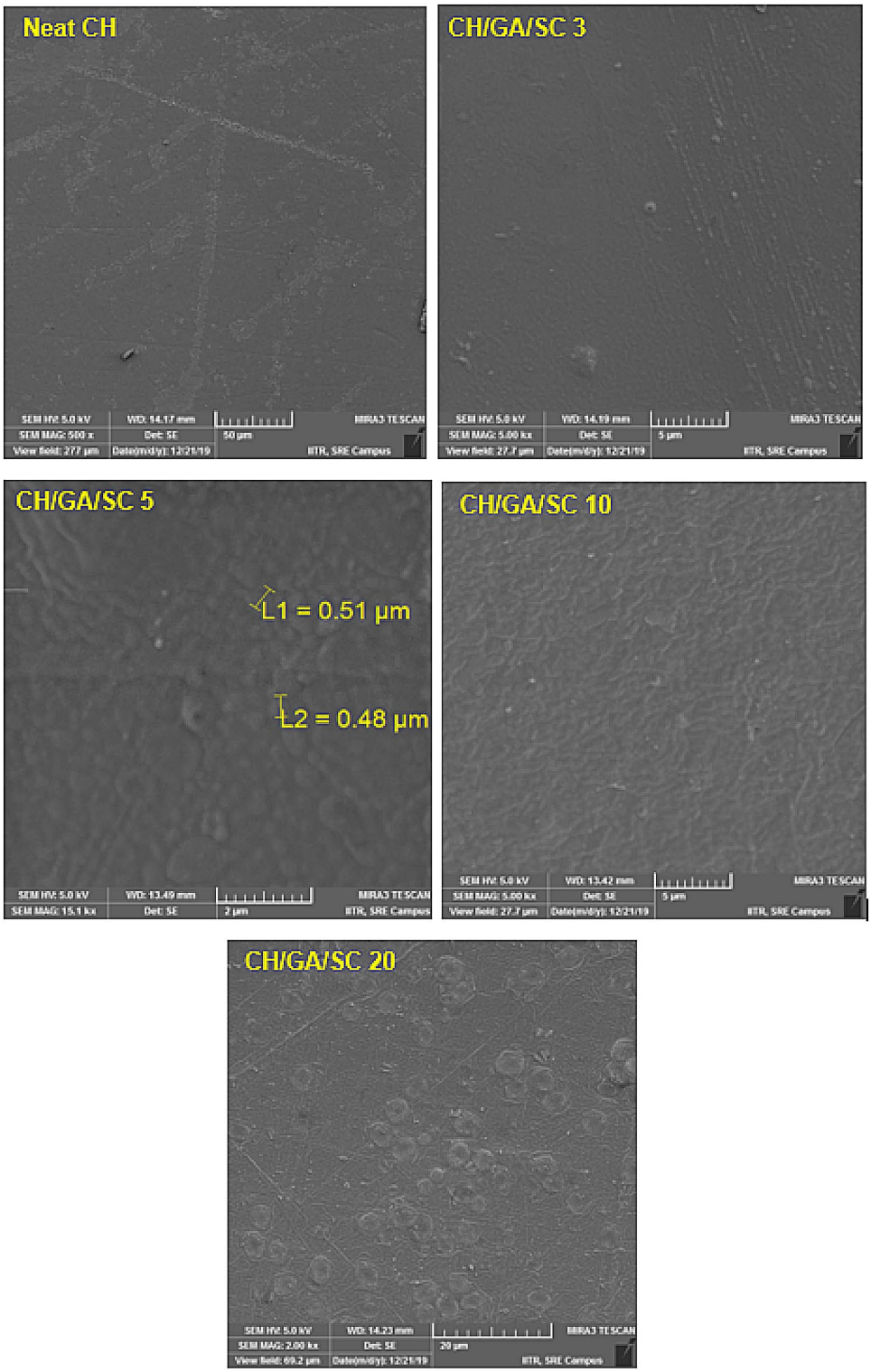

Fig. 3 SEM photographs of top surface of Neat CH and CH/GA/SC films

[29]. The gallic acid and sodium carbonate content affected the intermolecular hydrogen bonding, and the physical connection between chitosan, gallic acid, and glycerine, which lead to the rough surface structure of gallic acid grafted chitosan film films [30].

Mechanical properties of films

Mechanical properties such as TS and EB are vital properties of polymer-based packaging material since tolerable mechanical strength confirms the veracity of the packaging

material and its independence from small defects [31]. Table 2 demonstrate the mechanical properties of Neat CH and CH/GA/SC films. Alterations in the TS and EB of Neat CH and CH/GA/SC 1,3, 5, 10, and 20 were noticed and could be associated with the incorporation of SC and GA interrelating with CH and establishing new linkages that disturb film matrix. Neat CH film had TS and EB values of 15.43 ± 0.21 MPa and 29.71 ± 2.13% respectively. The addition of 1% and 5% (w/w) SC and GA into CH films significantly ($p < 0.05$) increased its TS property. The incorporation of a comparatively minor quantity of GA displayed the maximum TS among all test films, which could be accredited to the development of intermolecular hydrogen bonding among the $–NH_3(+)$ group of the CH backbone and the OH^- of GA [28]. Furthermore, the intermolecular hydrogen bonding among CH and GA could improve the crosslinking, resulting in decreases in the molecular movement and the free space in the CH film matrix [24]. Test sample CH/GA/SC 20 showed lowest TS, 8.45 ± 0.39 MPa; associated to the high quantity of GA and SC distributed in the CH which cracks the internal matrix of the CH film. Our results are in good agreement with Sun et al. [28], who reported, incorporation of a lower amount of gallic acid into chitosan structure TS increased significantly; however, it decreased with a high amount.

EB (%) of CH/GA/SC film was significantly ($p < 0.05$) decreased from 29.71 ± 2.13 to 14.98 ± 2.76% with the addition of SC and GA, indicating the interface among the carboxylic group of GA and SC and the amino group of CH, which would decrease the flexibility of the CH/GA/SC films. Sun et al. [28] reported, a decrease in EB (%) values of GA incorporated CH films, indicated the addition of GA into the CH film caused strong reaction between filler and CH matrix which declined EB by reducing the movement in CH structure. The mechanical properties, especially TS and EB of CH films, depending on various factors such as assay of chitosan utilized, the existence of glycerol as a plasticizer, and the temperature utilized for drying of the film [32]. A polyphenolic compound such as gallic acid can act as a plasticizer in the polymeric films which further improves the mechanical properties of the film [20].

Water solubility

Film solubility in water stated as the percentage of water-soluble substance present in the prepared CH films is common practice to designate the confrontation of the film with regards to water. The solubility of neat CH and CH/GA/SC active films in water is presented in Table 1. The solubility of Neat CH film in water was 22.65%. Nevertheless, the incorporation of GA into CH structure leads to a substantial rise in the percentage of water solubility ($p < 0.05$). The water solubility of CH/GA/SC active films increased from 22.81 to 32.56% with the increasing the amount of GA in CH films. The increase in the solubility of CH/GA/SC film in water could be credited to the hydrophilic nature of gallic acid molecules. Our results are in good agreement with Liu et al. [33], who stated that the water solubility percentage was increased when protocatechuic acid incorporated into chitosan for the development of chitosan–phenolic composite films. The water solubility of CH film could be reduced by the addition of hydrophobic molecules, for example, tannic acid or α-tocopherol into film-forming solution [29].

X-ray diffraction analysis

X-ray diffractograms of the Neat CH and CH/GA/SC active barrier films were noted for the assessment of the degree of crystallinity of the films. The crystalline and amorphous regions in the CH/GA/SC films were established from the diffractograms patterns. As presented in Fig. 4, the X-ray diffractogram of Neat CH film displayed diffractograms peaks at $2\theta = 9.4$, 12.7, and 15.2, associated with a semi-crystalline in the amorphous matrix of CH, which were comparable with an earlier study [33]. The peak at $2\theta = 18.4°$ was noticed in neat CH film prepared by dissolving CH in acetic acid solution during film preparation [27]. The broad peak at $2\theta = 23.4°$ associated with the amorphous nature of

Table 2 Thickness, mechanical and oxygen scavenging properties of Neat CH and CH/GA/SC films containing different concentrations of gallic acid

Sample	Thickness (mm)	Tensile strength (MPa)	Elongation at Break (%)	Oxygen scavenging efficiency (mL O_2/gm* day)	Oxygen scavenging capacity (mL O_2/g)
Neat CH	0.038 ± 0.006[a]	15.43 ± 0.21[c]	29.71 ± 2.13[a]	–	–
CH/GA/SC 1	0.039 ± 0.009[a]	19.50 ± 0.11[a]	29.26 ± 1.88[a]	0.27	1.82
CH/GA/SC 5	0.043 ± 0.007[b]	16.89 ± 0.76[b]	26.22 ± 0.42[b]	0.54	4.34
CH/GA/SC 10	0.048 ± 0.007[c]	12.01 ± 0.61[b]	20.68 ± 1.33[b]	1.38	11.06
CH/GA/SC 20	0.053 ± 0.007[c]	8.45 ± 0.39c	14.98 ± 2.76[c]	2.44	19.55

Values expressed as mean ± standard deviation

Different letters in the same column indicate significant differences ($p < 0.05$)

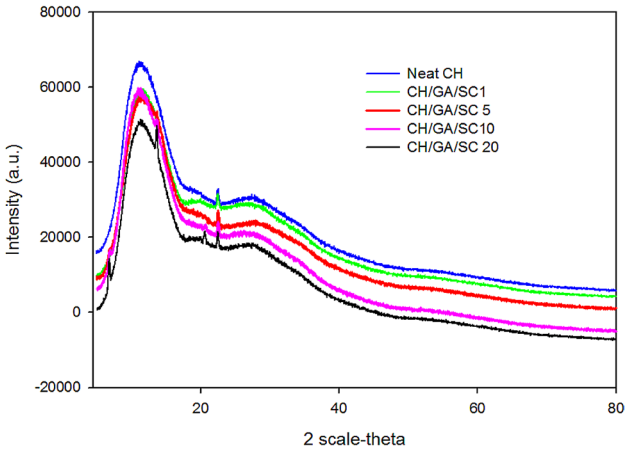

Fig. 4 X-ray diffraction pattern of chitosan films containing sodium carbonate and gallic acid

the CH film [29]. When SC and GA were added into the CH matrix, the crystalline peak of GA (15.7°), along with the hydrated crystalline peak of CH (8.5), didn't appear. The absence of these crystalline character peaks was possible as a result of the molecular interactions among CH, GA, and SC. The intensity of diffractograms peak at 22.7° was nearly the same for all tested film samples. However, this diffractogram peak was noticed to become weak and wide in CH/GA/SC active films added with gallic acid and sodium carbonate. This designated the crystalline characteristic of CH films was linked with the type and content of phenolic compounds incorporated [33].

WVP

The rate of water vapor moving across a polymeric film is combined with the rates of adsorption-desorption, and diffusion, where on one side of the film, water molecules get dissolve and move in the void space between film sides and further desorb from the film surface on the other side of the film. As presented in Table 1, the WVP values of prepared films ranged between 3.54 ± 1.23 and 2.31 ± 0.91 g mm/m^2 h kPa ($p < 0.05$). Riaz et al. (2018) described the WVP of the chitosan-based active film incorporated with polyphenols from apple peel in the range of $1.00–3.04 \times 10^{10}$ g m^{-1} Pa^{-1} s^{-1}. The CH/GA/SC 20 film attained the lowest WVP value confirming that the addition of GA and SC led to improve WVP of the prepared active barrier films. Improved WVP might be associated with the presence of the high amount of GA and SC in CH film structure; the film promotes internal rearrangement and delays permeability. With increasing the amount of GA in the CH matrix, lower the WVP of films, this is due to the large benzene ring group of GA hinders the intermolecular and intramolecular hydrogen bonding link of CH. [34]. The incorporation of polyphenols such as GA in the biodegradable polymeric film can develop hydrogen bonding and interactions of hydrophobic with the polar groups in the biodegradable polymer, hence, limit the quantity of free hydroxy group which could interact with a water molecule [35]. Our results are in good agreement with Pacheco et al. [34], who reported, chitosan and starch-based packaging film containing varying amount of GA showed improved WVP with the increasing amount of gallic acid.

Oxygen permeability of activated films

Oxygen is an important factor in the lipid oxidation process, which further reduces the physical and nutritional quality of food products and hence minimize the shelf life [20]. Table 2 shows the oxygen permeability of activated CH/GA/SC films. The OP of neat CH film was 6.21 ± 1.23 cm^3/µm/m^2 day kpa, which indicates that the film had an acceptable oxygen barrier limit for food packaging applications. With increasing concentration of GA and SC in CH structure, OP decreased from 6.21 ± 1.23 to 4.10 ± 1.07 cm^3/µm/m^2 day kpa. A significant ($p < 0.05$) improvement in the barrier properties of CH/GA/SC films which can be attributed to the decrease in the tortuosity of the diffusive path for the oxygen to diffuse through the prepared film. On the other hand, oxygen permits through the film were scavenged by the active oxygen scavenging layer made using GA and SC in the film. Our results are in good agreement with Sun et al. [28], who reported, oxygen permeability of chitosan–gallic acid film was improved as 0.56 ± 0.06 and 0.90 ± 0.03 (mol m^{-1} s^{-1} Pa^{-1}) $\times 10^{-18}$ with the addition of 0.5 g/100 g and 1 g/100 g into chitosan film-forming solution respectively. The integration of GA into polymeric films plays an significant role in the enhancement of oxygen permeability [28].

Oxygen-scavenging properties of films

The oxygen scavenging rate and capacities of the neat CH and CH/GA/SC films with the increasing quantity of GA presented in Table 2. The oxygen content present in the glass flask containing the CH/GA/SC films reduced in all test flask during 8 days of storage time. The CH/GA/SC 20 film displayed the maximum oxygen scavenging capacity compared to other test samples. The oxygen scavenging rate and capacity was 2.44 mL O_2/g day and 19.55 mL O_2/g after 8 days. With reducing the content of GA in C films, the oxygen scavenging performance also reduced. Our results could be comparable with conventional oxygen scavenger used for food packaging; for instance, 6.72 mL O_2/g scavenger for alpha-tocopherol containing oxygen absorbers (Byun et al. 2011). Oxygen scavenging efficiency of CH/GA/SC 5, 10 films exhibited 0.54, 1.38 mL O_2/g day, respectively, and oxygen scavenging capacity of CH/GA/SC 5 and 10 films was 4.34 and 11.06 mL O_2/g respectively. Our results are

in good agreement with Shin et al. [36], who reported, the oxygen-absorbing films manufactured by incorporation of iron as an oxygen scavenger into the LDPE matrix exhibited 6.10 mL O_2/g scavenging capacity by 50% iron incorporated film sample. Here, relative humidity began the oxygen scavenging reaction in the CH/GA/SC films. The water molecule reacts with SC and generates an alkaline atmosphere, and GA in an alkaline atmosphere initiates reacting with oxygen existing in the headspace of the glass flask. Gallic acid is a multipurpose scavenger capable of speedily deactivating an extensive variety of reactive oxygen species (ROS) through electron transfer at physiological pH [9], CH/GA/SC 10 and 20 film samples exhibited suitable oxygen scavenging properties, which is an essential parameter for their application as oxygen scavenging packaging material for food products [4]. Our results prove that the prepared active barrier films CH/GA/SC10 and 20% GA can be used as a prominent active barrier with oxygen scavenging materials for the packaging of high water activity food products.

Conclusion

Active oxygen barrier CH/GA/SC films were prepared via a solution casting method. The CH–GA–SC ratios in the matrix displayed a significant impact on the physicochemical properties of films.. Sodium carbonate used as an activator in the oxygen scavenging reaction upon moisture activation; prepared films to perform as oxygen scavenging packaging material and offer both oxygen absorbance and rapid oxidation kinetics. Therefore, these active oxygen barrier films are predominantly appropriate for food packaging applications. Prospects in this particular research area may be found in exploring the potential use of CH/GA/SC films for packaging numerous oxygen-sensitive food products. Therefore, GA and SC incorporated CH films seem to be a capable and improved substitute for the polymeric packaging material for the food.

Acknowledgements This project supported by Department of Science and Technology (DST), Government of India, for the financial support provided under DST INSPIRE Faculty (Grant No. DST/INSPIRE/04/2018/002544).

References

1. K.K. Gaikwad, S. Singh, Y.S. Negi, Environ. Chem. Lett. **18**, 269–284 (2020)
2. S. Singh, K.K. Gaikwad, Y.S. Lee, Sci. Hortic. **256**, 108548 (2019)
3. S. Singh, K.K. Gaikwad, Y.S. Lee, Korean J. Packag Sci. Technol. **24**, 167–180 (2018)
4. K.K. Gaikwad, S. Singh, J. Shin, Y.S. Lee, LWT-Food Sci. Technol. **117**, 108643 (2020)
5. S. Jafarzadeh, S.M. Jafari, A. Salehabadi, A.M. Nafchi, U.S. Uthaya, H.A. Khalil, Trends Food Sci. Technol. **100**, 262–277 (2020)
6. S. Singh, K.K. Gaikwad, Y.S. Lee, J. Therm. Anal. Calorim. **139**, 1915–1923 (2020)
7. A. Ashrafi, M. Jokar, A.M. Nafchi, Int. J. Biol. Macromol. **108**, 444–454 (2018)
8. B.J. Ahn, K.K. Gaikwad, Y.S. Lee, J. Appl. Polym. Sci. **133**, 43 (2016)
9. K.K. Gaikwad, S. Singh, Y.S. Lee, Environ. Chem. Lett. **16**, 523–538 (2018)
10. W.S. Choi, S. Singh, Y.S. Lee, LWT-Food Sci. Technol. **70**, 213–222 (2016)
11. N. Faas, B. Röcker, S. Smrke, C. Yeretzian, S. Yildirim, Food Packag. Shelf Life **24**, 100488 (2020)
12. K.K. Gaikwad, S. Singh, Y.S. Negi, Y.S. Lee, Food Meas. **14**, 1857–1864 (2020)
13. A. Dey, S. Neogi, Trends Food Sci. Technol. **90**, 26–34 (2019)
14. S. Singh, K.K. Gaikwad, M. Lee, Y.S. Lee, Food Meas. **12**, 588–601 (2018)
15. L. Yu, Y.S. Lim, J.H. Han, K. Kim, J.Y. Kim, S.Y. Choi, K. Shin, Synth. Met. **162**, 710–714 (2012)
16. Y. Wang, M. Shoda, A. Hisama, K. Oyaizu, H. Nishide, Macromol. Chem. Phys. **220**, 1900294 (2019)
17. M. Ghasemlou, F. Khodaiyan, A. Oromiehie, Carbohydr. Polym. **84**, 477–483 (2011)
18. D. Alkan, L.Y. Aydemir, I. Arcan, H. Yavuzdurmaz, H.I. Atabay, C. Ceylan, A. Yemenicioglu, J. Agric. Food Chem. **59**, 11003–11010 (2011)
19. Y. Byun, D. Darby, K. Cooksey, P. Dawson, S. Whiteside, Food Chem. **124**, 615–619 (2011)
20. K. Limpisophon, G. Schleining, J. Food Sci. **82**, 80–89 (2017)
21. I. Zarandona, A.I. Puertas, M.T. Dueñas, P. Guerrero, K. de la Caba, Food Hydrocolloids **101**, 105486 (2020)
22. K.K. Gaikwad, J.Y. Lee, Y.S. Lee, J. Food Sci. Technol. **53**, 1608–1619 (2016)
23. L. Wang, Y. Dong, H. Men, J. Tong, J. Zhou, Food Hydrocolloids **32**, 35–41 (2013)
24. M. Rezaee, G. Askari, Z. Emam Djomeh, M. Salami, Int. J. Biol. Macromol. **114**, 844–850 (2018)
25. L. Rui, M. Xie, B. Hu, L. Zhou, D. Yin, X. Zeng, Carbohydr. Polym. **173**, 473–481 (2017)
26. S.B. Schreiber, J.J. Bozell, D.G. Hayes, S. Zivanovic, Food Hydrocolloids **33**, 207–214 (2013)
27. X. Zhang, J. Liu, C. Qian, J. Kan, C. Jin, Food Hydrocolloids **89**, 1–10 (2019)
28. X. Sun, Z. Wang, H. Kadouh, K. Zhou, LWT-Food Sci. Technol. **57**, 83–89 (2014)
29. V. Rubentheren, T.A. Ward, C.Y. Chee, P. Nair, Cellulose **22**, 2529–2541 (2015)
30. C. Wu, Y. Li, L. Wang, Y. Hu, J. Chen, D. Liu, X. Ye, Food Bioprocess. Technol. **9**, 675–685 (2016)
31. S. Singh, P.K. Maji, Y.S. Lee, K.K. Gaikwad, Environ. Chem. Lett. (2020). https://doi.org/10.1007/s10311-020-01085-8
32. M. Pereda, G. Amica, N.E. Marcovich, Carbohydr. Polym. **87**, 1318–1325 (2012)
33. J. Liu, S. Liu, Q. Wu, Y. Gu, J. Kan, C. Jin, Food Hydrocolloids **73**, 90–100 (2017)
34. N. Pacheco, M.G. Naal-Ek, T. Ayora-Talavera, K. Shirai, A. Román-Guerrero, M.F. Fabela-Morón, J.C. Cuevas-Bernardino, Int. J. Biol. Macromol. **125**, 149–158 (2019)
35. M.J. Fabra, I. Falcó, W. Randazzo, G. Sánchez, A. López-Rubio, Food Hydrocolloids **81**, 96–103 (2018)
36. Y. Shin, J. Shin, Y.S. Lee, Macromol. Res. **19**, 869 (2011)

Publisher's Note Springer Nature remains neutral with regard to jurisdictional claims in published maps and institutional affiliations.